Geophys. J. R. astr. Soc. (1972) **31**, 141–161.

Tectonic Strain Release by Underground Nuclear Explosions and its Effect on Seismic Discrimination

M. Nafi Toksöz and Harold H. Kehrer

(Received 1972 April 24)*

Summary

The analysis of surface waves from a large number of underground nuclear explosions reinforces the hypothesis of tectonic strain release. Such strain release is dependent on rock type and ambient stress levels. In harder media, such as granite, strain release is considerably greater than in soft media such as loose alluvium and salt. In the case of three events for which the tectonic component exceeded that of the explosion itself, the effect on the $M_s - m_b$ discriminant due to the added surface wave energy was not noticeable. This was probably due to the averaging of magnitude over all azimuths. A decaying pulse-type source-time function is consistent with surface wave amplitude spectra and can explain the long-period/short-period spectral ratio.

1. Introduction

The source mechanisms of underground nuclear explosions have been of great seismological interest since it was first observed that a pure explosive source alone could not adequately account for the radiation patterns of seismic waves recorded at distant stations. Most notable among these observations are the presence of *SH* and Love waves and azimuthal asymmetry of the Rayleigh wave radiation patterns. There have been a number of studies dealing with the radiation patterns and the generation of *SH*-type seismic waves by underground nuclear explosions (Press & Archambeau 1962; Brune & Pomeroy 1963; Aki 1964; Toksöz, Ben-Menahem & Harkrider 1964, 1965; Toksöz 1967; Archambeau 1968; Kehrer 1969; Molnar, Jacob &Sykes 1969; Archambeau & Sammis 1970; Toksöz & Kehrer 1971; Toksöz, Thomson & Ahrens 1971). It is generally accepted that the Love waves are generated at or very near the source and that they may be associated with the release of tectonic strain energy by the explosion. As recent calculations by Leavy (1971) show, near-source inhomogeneities and scattering cannot account for the observed amplitudes of Love waves. Geological studies (McKeown *et al.* 1966; Barosch 1968; Bucknam 1969; McKeown & Dickey 1969; Dickey 1968, 1969, 1971) clearly indicate fault movements and surface displacements associated with the majority of explosions. Aftershocks that follow the explosions (Hamilton & Healy 1969; Ryall & Savage 1969; Stauder 1971) generally resemble the sequence that follows earthquakes and they indicate the disturbance of the regional tectonic stress patterns by the explosion.

When observed outside the source region, seismic waves which are due to a tectonic strain release component will have spectral properties and radiation patterns

* Received in original form 1972 April 12

similar to those of an earthquake. These will be superimposed on waves radiated isotropically by the pure explosive source. The questions that arise are: (1) What is the extent of tectonic strain energy release?, and (2) How significantly does this complication affect some of the seismic discriminants such as $M_s - m_b$ relationships? In this paper we address ourselves to these points.

The paper is divided into three parts. In Part I, we present the strain release characteristics of about 20 underground explosions. For this, we use Rayleigh wave radiation patterns as well as Love-to-Rayleigh wave amplitude ratios. We show the importance of medium properties and tectonic framework in controlling the energy release. In Part II, we evaluate the effect of the released strain energy on the surface wave magnitudes. Part III is devoted to a somewhat separate subject—the source function of the explosion. A decaying pulse-type pressure function fits the observed surface spectra and explains the success of some of the spectral ratio discriminants.

2. Tectonic strain release characteristics of explosions

Examples of Rayleigh and Love waves generated by three explosions are shown in Fig. 1. These illustrate the differences in the relative generation of Love waves by NTS (Nevada Test Site) explosions recorded at Weston, Massachusetts. Love waves appear on the tangential components (T), about 2 min earlier than the Rayleigh waves on the vertical components (Z). The large amplitude of Love waves relative to Rayleigh waves for Pile Driver and Greeley indicates the greater amount of tectonic strain release by these explosions.

To determine the contribution of strain release on the radiated wave, we formulate a composite source consisting of a pure explosion plus a double-couple component representing the strain release. For such a source, the theoretical formulations for the azimuthal dependence of Rayleigh wave amplitudes and Love/Rayleigh amplitude

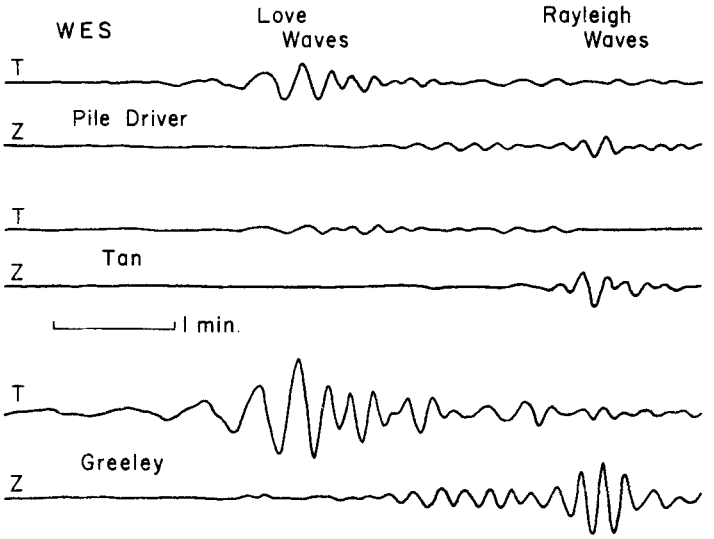

FIG. 1. Long-period filtered seismograms from the Pile Driver, Tan, and Greeley explosions recorded at Weston, Massachusetts.

ratios can be written as (Toksöz, Harkrider & Ben-Menahem 1965; Toksöz *et al.* 1971; Kehrer 1969):

$$\left.\begin{aligned} U_{Rz} &= W_e\left(1+F\left(\tfrac{1}{2}\sin\lambda\sin 2\delta\left(\frac{1+\sigma_0}{1-\sigma_0}-\cos 2\theta\right)+\cos\lambda\sin\delta\sin 2\theta\right)\right) \\ \frac{|U_{L\theta}|}{|U_{Rz}|} &= \frac{Fk_L^{\frac{1}{2}}A_L(\tfrac{1}{2}\sin\lambda\sin 2\delta\sin 2\theta+\cos\lambda\sin\delta\cos 2\theta)}{\left(1+F\left(\tfrac{1}{2}\sin\lambda\sin 2\delta\left(\frac{1+\sigma_0}{1-\sigma_0}-\cos 2\theta\right)+\cos\lambda\sin\delta\sin 2\theta\right)\right)k_R^{\frac{1}{2}}A_R\left(\frac{\dot{u}_0{}^*}{\dot{w}_0}\right)} \\ &\qquad \exp\left(-r(\gamma_L-\gamma_R)\right) \end{aligned}\right\} \quad (1)$$

where W_e is the vertical component of displacement due to the explosive source; A_R and A_L are the Rayleigh and Love amplitude factors (Harkrider 1964); k_R and k_L are the Rayleigh and Love wave numbers; $\dot{u}_0$ and $\dot{w}_0$ are components of particle velocity at the surface; σ_0 is Poisson's ratio at the surface; γ_R and γ_L are the Rayleigh and Love wave attenuation coefficients: δ and λ are the dip and slip directions of the fault plane: θ is its azimuth; and F is the strength of the double-couple relative to the explosion. In equation (1), the difference in explosion and earthquake source time functions and source dimensions are considered negligible for a narrow frequency band. Over a broader period range (i.e. 10–60 s), the differences are determined from the data as discussed later in this Section and in Section 4.

For a horizontal double couple, $\delta = 90°$ and $\lambda = 0°$ and we obtain

$$\left.\begin{aligned} |U_{Rz}| &= W_e(1+F\sin 2\theta) \\ \frac{|U_{L\theta}|}{|U_{Rz}|} &= \frac{Fk_L^{\frac{1}{2}}A_L\cos 2\theta}{(1+F\sin 2\theta)k_R^{\frac{1}{2}}A_R\left(\frac{\dot{u}_0{}^*}{\dot{w}_0}\right)}\exp\left(-r(\gamma_L-\gamma_R)\right) \end{aligned}\right\} \quad (2)$$

In this study we use equation (2) to determine the strength of the double couple (F value) and the orientation of the double couple (θ) from Rayleigh wave amplitudes and Love/Rayleigh amplitude ratios. Other quantities are computed theoretically for specified layered Earth models (Harkrider 1964). The reasons for choosing the strike-slip model are: (1) The largest contribution to Love wave radiation comes from the strike-slip component of motion, and (2) The number of parameters to be estimated is reduced from four to two. With four parameters, the best-fitting radiation pattern cannot be uniquely determined.

Long-period seismograms were obtained from stations throughout North America for the study of the U.S. explosions. These included stations of the World Wide Standard Seismograph Network (WWSSN), the Long Range Seismic Measurements Network (LRSM), the Canadian Standard Seismograph Network (CSSN), and two additional stations at Berkeley and Pasadena which provided long-period data. Fig. 2 shows the distribution of recording stations in North America. However, not all stations provided useful data for each event. For the presumed Soviet events, data was obtained from the WWSSN stations in Europe and Asia.

The film records of those events, for which the surface wave data were of sufficient quality, were digitized, band-pass filtered (8–60 s) to reduce noise, and the two horizontal components were rotated to radial and tangential directions with respect

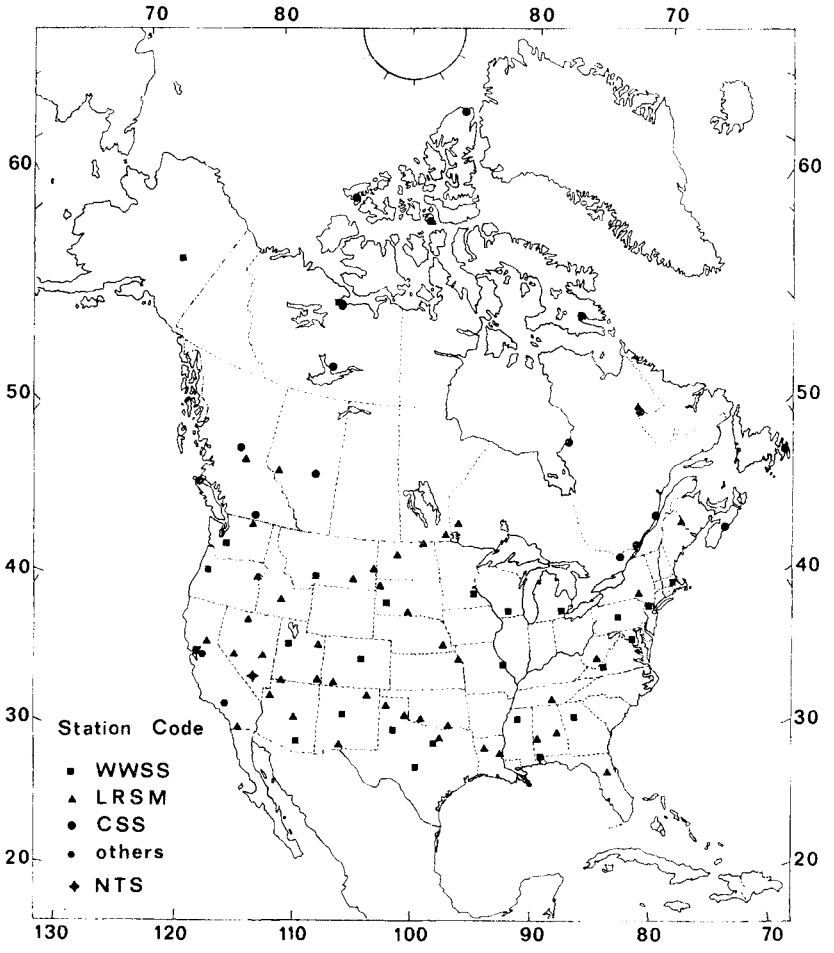

FIG. 2. Stations recording surface waves from explosions in the continental United States.

to the epicentre. In this way essentially pure Love waves were obtained on the tangential component. Fig. 3 is an example of this analysis for the explosion Boxcar recorded at Mould Bay, Canada. The three lower traces are plotted from digital data and show the unfiltered north–south, east–west, and vertical components. The three upper traces show the filtered data, where the horizontal components have been rotated to radial and tangential directions.

The tangential and the vertical components were then Fourier-analysed to yield the amplitude spectra. The proper time windows for this analysis were determined by examining the filtered trace at each station individually and noting the onset and duration of the wave trains.

Love wave to Rayleigh wave amplitude ratios were determined by computing the spectral ratio of the tangential component to the vertical component over the period range 8–60 s. In general, the spectral ratios were somewhat oscillatory and thus the ratio at any one particular period could not be expected to be reliable at all stations. The period range was, therefore, divided into three bands, from 9 to 15 s, from 15 to 22 s, and from 22 to 30 s. The average value of the ratio in each band was then taken to represent the ratio over that band.

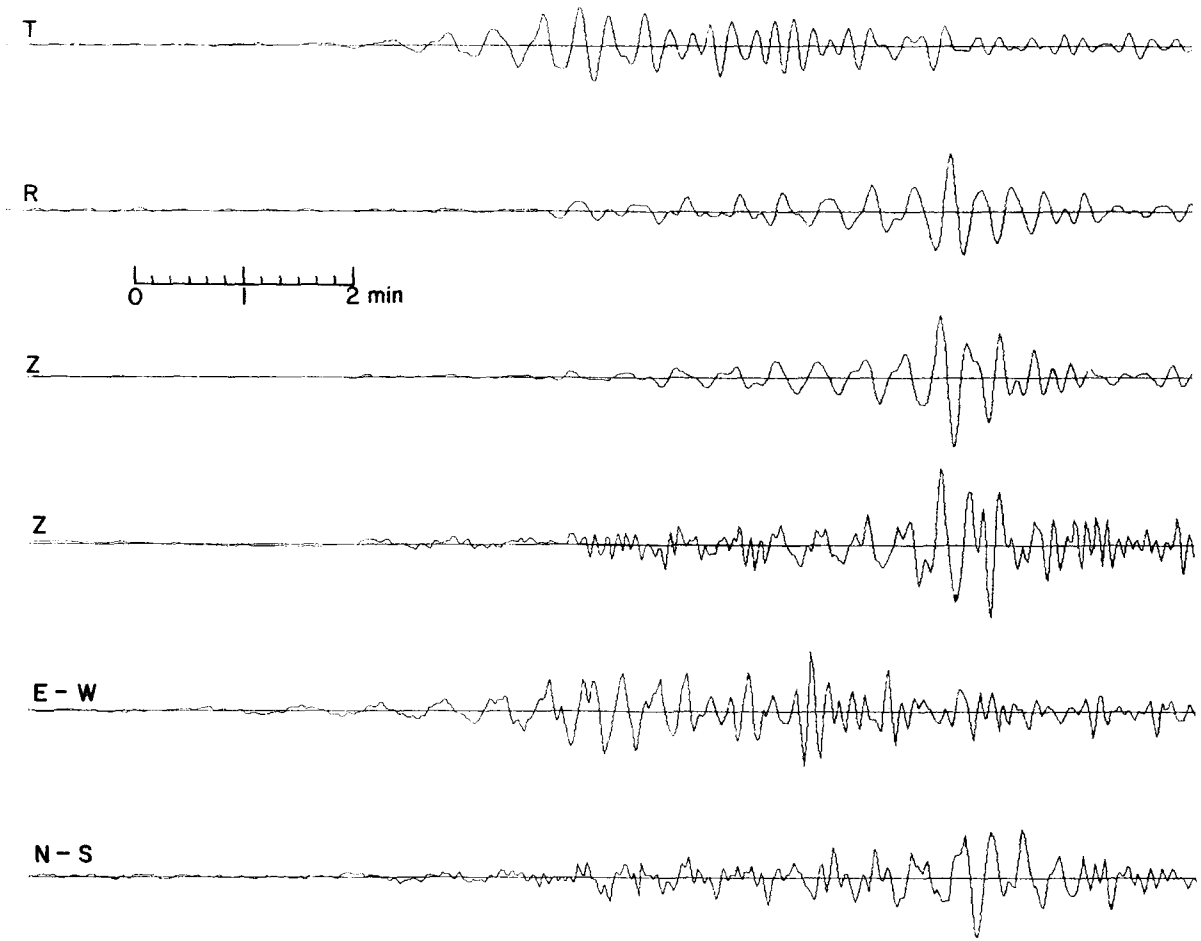

FIG. 3. Filtered (upper three traces) and unfiltered (lower three traces) long-period components from the Boxcar explosion at Mould Bay, Canada (MBC) plotted from digital data at the same gain. The two filtered horizontal components have been rotated to radial and tangential directions to separate Love and Rayleigh waves.

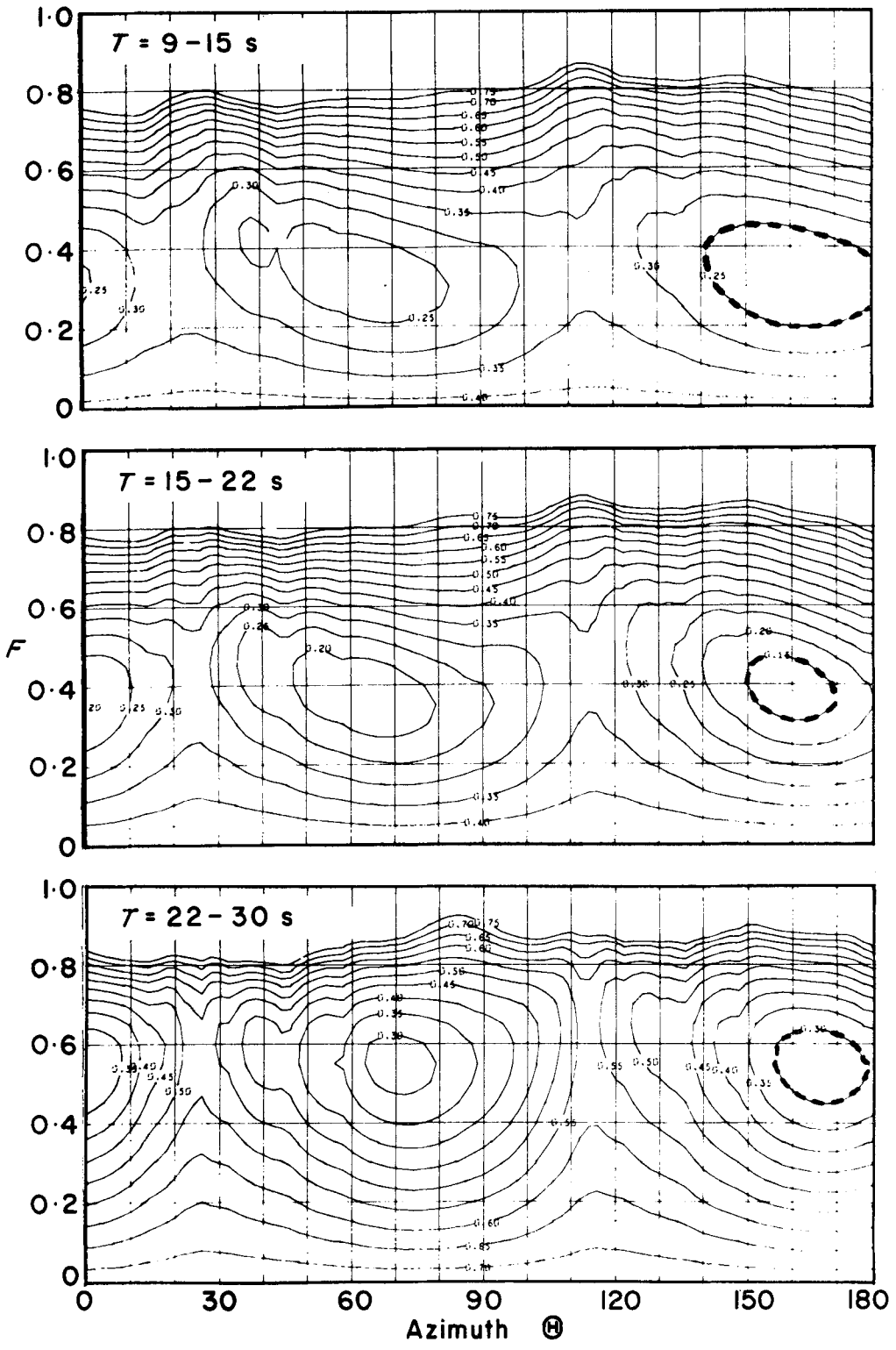

FIG. 4. Contour plots of the deviations of combinations of part double couple and fault plane azimuth from experimental Love to Rayleigh wave ratios for three period ranges: (a) 9–15 s, (b) 15–22 s, and (c) 22–30 s, for the Tan event. The centres of the minimum contours (broken curves) were taken to correspond to the best fitting combination of F and θ in each period band

An automatic error scheme (Kehrer 1969) was used to determine the best fit of equation (2) to the observed data. In applying equation (2), the term $k_L^{\frac{1}{2}} A_L/k_R^{\frac{1}{2}} A_R(\dot{u}_0^*/\dot{w}_0)$ was taken to be a constant at all stations, since for a near surface source, the Love/Rayleigh wave amplitude ratio changes very little with structure over continental paths (see Canitez & Toksöz 1971, Fig. 1). An error term E was then formed between the observed and the theoretical ratios for combinations of F and θ.

$$E_j = \left(\sum_{i=1}^{N} \left(\frac{L_i}{R_i} - \left| \frac{S.F_j \cos 2\theta_{ij}}{1 + F_j \sin 2\theta_{ij}} \right| \right)^2 \Big/ N \right)^{\frac{1}{2}} \tag{3}$$

The jth combination of F and θ which fits the data best will be that which minimizes E. L_i/R_i is the experimentally measured Love wave to Rayleigh wave amplitude ratio at a particular station i, S is a constant, and N is the number of stations. The values of E were contoured on a Stromberg–Carlson 4020 grid for the three period-bands of each event. Fig. 4 shows these results for the explosion Tan. The minima indicate the orientation of the best fitting right-lateral, vertical, strike-slip fault as measured clockwise from the north at the source. A comparison of the error plots over the three bands in Fig. 4 reveals the frequency dependence of F. The orientation θ of the double couple remains essentially unchanged over the three bands while F is greatest at long periods and smallest at short periods. This relationship was observed for nearly all events and indicates that the source of Love wave is less efficient at short periods than the Rayleigh wave source. A similar phenomenon was noted by Aki *et al.* (1969) for body waves from the Benham event. Fig. 5 shows the relationship between F and period for several events.

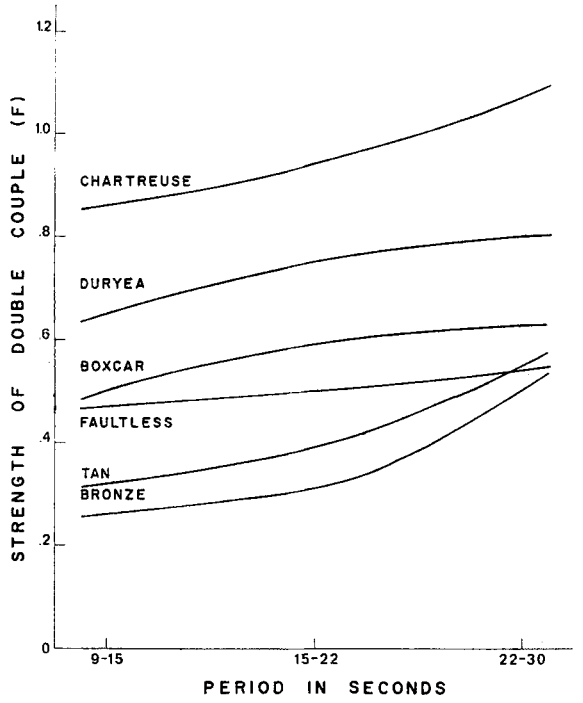

FIG. 5. The period dependence of F, the part double-couple, for six nuclear explosions.

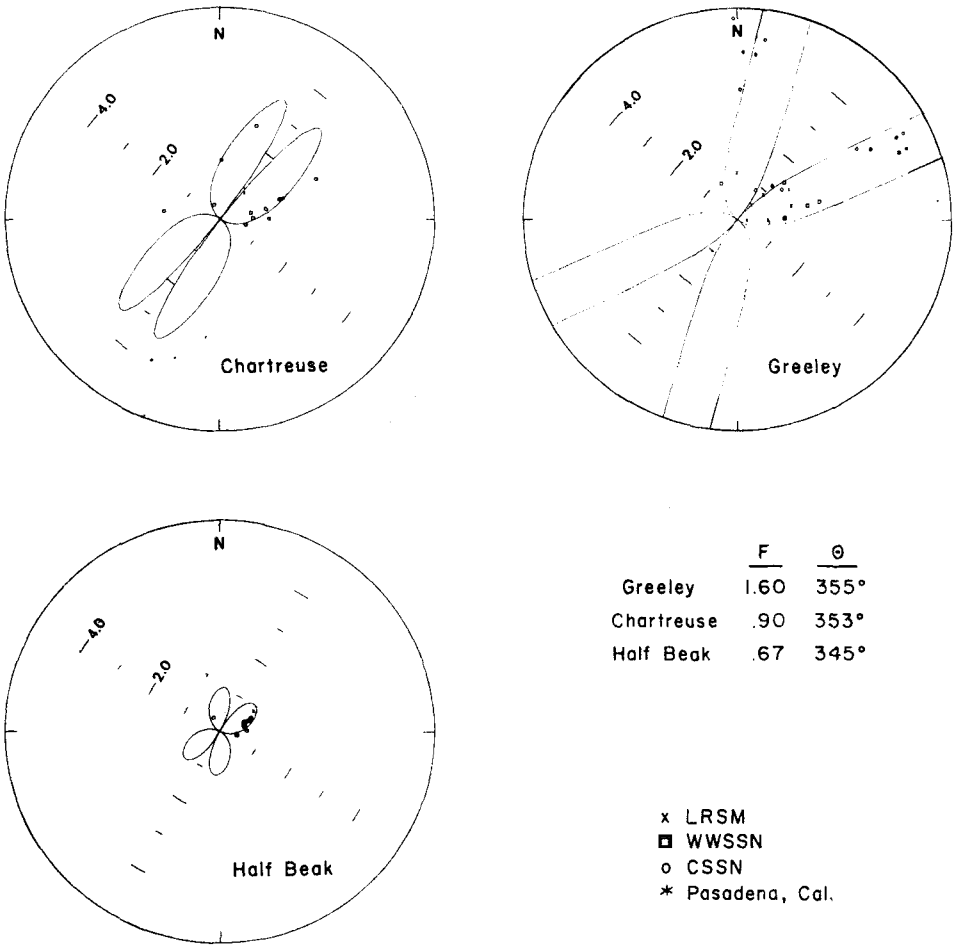

FIG. 6. Observed and theoretical Love/Rayleigh wave amplitude radiation patterns for three explosions with different proportions of strain release (F).

Observed and calculated Love/Rayleigh amplitude ratios as a function of azimuth for three explosions are shown in Fig. 6. A summary of the best fitting F and θ in the 15- to 22-s period range for each event is given in Table 1. For some explosions (Buff and the presumed Soviet events of 1966.3.20, 1967.3.26 and 1967.10.21) for which the surface wave data was not of sufficient quality to permit the calculation of spectral ratios, the parameters F and θ were determined from measurements of the maximum amplitudes of Love and Rayleigh waves. Included in Table 1 is the ratio of the surface wave energy of the double couple to the energy of the explosion. This ratio (Toksöz, Harkrider & Ben-Menahem 1965) is closely approximated by

$$E_{tect}/E_{exp} = 4/3F^2. \tag{4}$$

Several conclusions can be drawn from Table 1. The close agreement in fault orientation of the events at the Nevada Test Site indicates that a regional stress field is probably controlling the strain release. The large variation within the two Soviet testing areas may be due to a lack of sufficient data in the case of three of the events. The dependence of F and hence the amount of stress release, on lithology was previously noted by Toksöz (1967) and by Toksöz & Kehrer (1971). Table 1 provides

Table 1

Tectonic strain release characteristics of underground nuclear explosions

Event	Date	Region	Medium	D.C. Strength (F)	Fault Azi.	Energy ratio E_{tect}/E_{exp}
Pile Driver	1966.6.2	Yucca Flat (n. end)	Granite	3·20	340°	13·65
Hardhat	1962.2.15	Yucca Flat (n. end)	Granite	3·00	330°	12·00
Shoal	1963.10.26	Fallon, Nevada	Granite	0·90	346°	1·05
Greeley	1966.12.20	Pahute Mesa	Zeolite Tuff	1·60	355°	3·41
Benham	1968.12.19	Pahute Mesa	Zeolite Tuff	0·85	345°	0·96
Chartreuse	1966.5.6	Pahute Mesa	Rhyolite	0·90	353°	1·05
Duryea	1966.4.14	Pahute Mesa	Rhyolite	0·75	355°	0·75
Half Beak	1966.6.30	Pahute Mesa	Rhyolite	0·67	345°	0·60
Boxcar	1968.4.26	Pahute Mesa	Rhyolite	0·59	346°	0·46
Corduroy	1965.12 3	Yucca Flat	Quartzite	0·72	347°	0·69
Rulison	1969.9.10	Grand Valley, Colorado	Ss. and Shale	0·60	335°	0·48
Faultless	1968.1.19	Central Nevada	Sat. Tuff	0·50	344°	0·33
Cup	1965.3.26	Yucca Flat	Tuff	0·55	200°	0·40
Bilby	1963.9.13	Yucca Flat	Tuff	0·47	340°	0·29
Tan	1966.6.3	Yucca Flat	Tuff	0·39	347°	0·20
Bronze	1965.7.23	Yucca Flat	Tuff	0·33	185°	0·15
Buff	1965.12.16	Yucca Flat	Tuff	0·31	208°	0·13
Haymaker	1962.6.27	Yucca Flat	Alluvium	0·33	340°	0·14
Sedan	1962.7.6	Yucca Flat	Alluvium	0	—	0
Salmon	1964.10.22	Hattiesburg, Mississippi	Salt	0	—	0
Gnome	1961.12.10	Carlsbad, New Mexico	Salt	0	—	0
Milrow	1969.10.2	Amchitka	Andesite	$<0·6$	—	$<0·48$
Cannikin	1971.11.6	Amchitka	Andesite	0·60	60°	0·48
U.S.S.R.	1966.10.27	Novaya Zemlya	—	0·90	5°	1·05
U.S.S.R.	1967.10.21	Novaya Zemlya	—	0·71	43°	0·67
U.S.S.R.	1967.2.26	E. Kazakh	—	0·85	6°	0·96
U S.S.R.	1967.3.20	E. Kazakh	—	0·81	155°	0·87
U.S.S.R.	1966.2.13	E. Kazakh	—	0·67	101°	0·60

additional evidence that the multipolar source component is larger in more competent rock. Thus strain release from a particular explosion is dependent on the rock medium and the regional state of strain. It is also apparent that there are variations for a given rock type, as in the case of the three events in granite. This can be explained by the differences in ambient stress levels and available strain energy (Toksöz *et al.* 1971). When the F value exceeds unity the Rayleigh wave radiation pattern will show a lobate structure and reversed polarity in alternating quadrants. This has been discussed in an earlier paper (Toksöz & Kehrer 1971) and is here demonstrated in Fig. 7 for the Pile Driver and Greeley explosions.

The north-north-west orientation of the fault planes of most of the Nevada Test Site explosions is in good agreement with lineaments and dominant fault patterns in the area. Fig. 8 shows the Yucca Flat portion of the Nevada Test Site with the source mechanisms of the explosions studied there. Included are the major natural faults and some of the fractures produced by the events. The chief feature of Yucca Flat is the Yucca Fault which trends northward through alluvium and is of recent age. Although most observed displacements across the Yucca Fault are vertical following nearby explosions, numerous *en echelon* fractures along the fault were produced

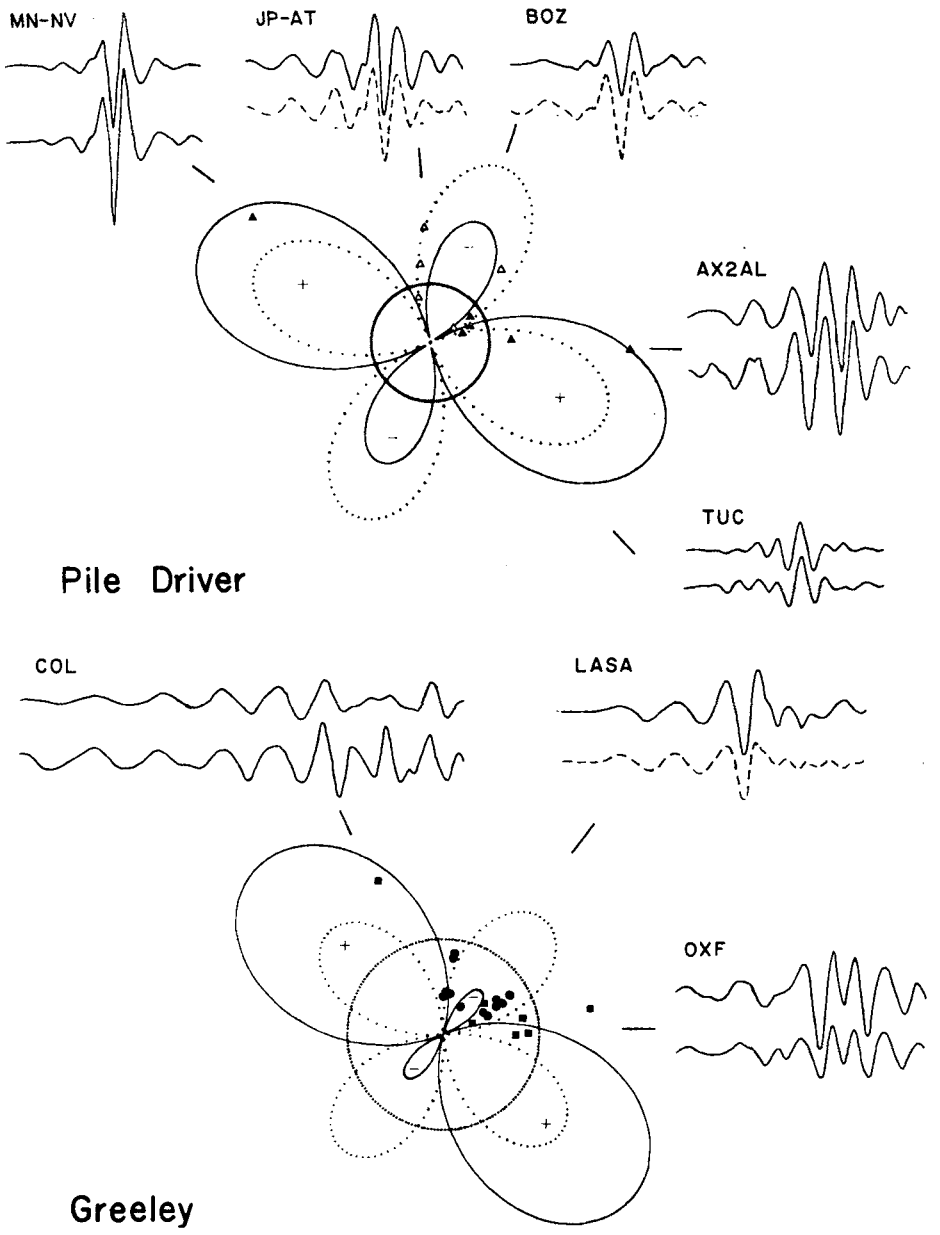

FIG. 7. Rayleigh wave radiation patterns for explosive component (circles), strain release component (broken curves), and composite sources representing the theoretical models (solid curves, where for Pile Driver: $F = 3{\cdot}2$ and $\theta = 340°$; and for Greeley: $F = 1{\cdot}6$ and $\theta = 355°$). The polarity (phase) of Rayleigh waves in different quadrants of the radiation pattern is indicated by (+) and (−). For Pile Driver some sample seismograms from four stations are compared to those of Tan. Amplitude factors are arbitrary. Pile Driver traces are below those of Tan. Dashed line traces have their polarities reversed. Note the perfect match of wave shapes, with polarities reversed at JP-AT and BOZ as predicted by the model. For Greeley sample seismograms are compared to those of Half Beak (COL and OXF) and Boxcar (LASA). The lower traces are from Greeley. Polarity reversal is very clear at LASA. MN-NV, Mina, Nev.; JP-AT, Jasper, Alta.; BOZ, Bozman, Mont.; AX2AL; Alexander City, Ala.; TUC, Tucson, Ariz.; COL, College, Alaska; LASA, Large Aperture Seismic Array, Mont.; OXF, Oxford, Miss. Data symbols: ▲, LRSM stations; △, LRSM stations where reversed polarity was observed; ■, WWSSN stations; ●, CSSN stations.

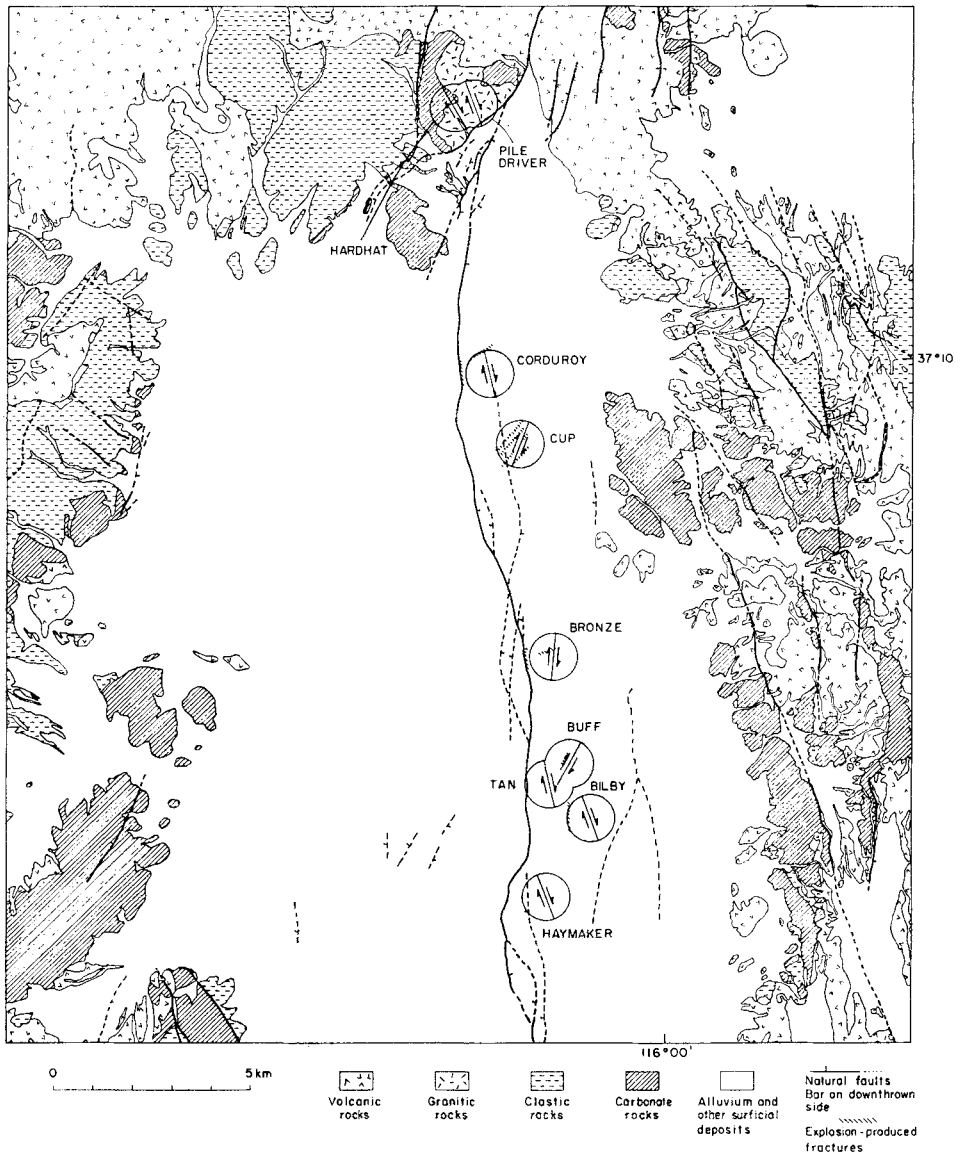

FIG. 8. Map of Yucca Flat showing the fault plane orientation of the explosions studied, explosion-produced fractures, and major natural faults in the area (geology after Fernald, Corchary & Williams 1968).

in the alluvium by Corduroy (Barosch 1968). Such an *en echelon* pattern is generally related to strike-slip movement in the underlying basement. The trend of the pattern in this case suggests right-lateral slippage.

Fig. 9 shows the Pahute Mesa portion of the Nevada Test Site with the natural faults, explosion-produced fractures, and the events studied. The main structural feature of Pahute Mesa is the Silent Canyon Caldera, which encloses the five events. Many normal faults, striking north-north-west, cut the thick sequence of Tertiary volcanic rock. Recent natural movement along some of these faults has been inferred (McKeown *et al.* 1966). For Benham and Boxcar, studies of aftershock distribution

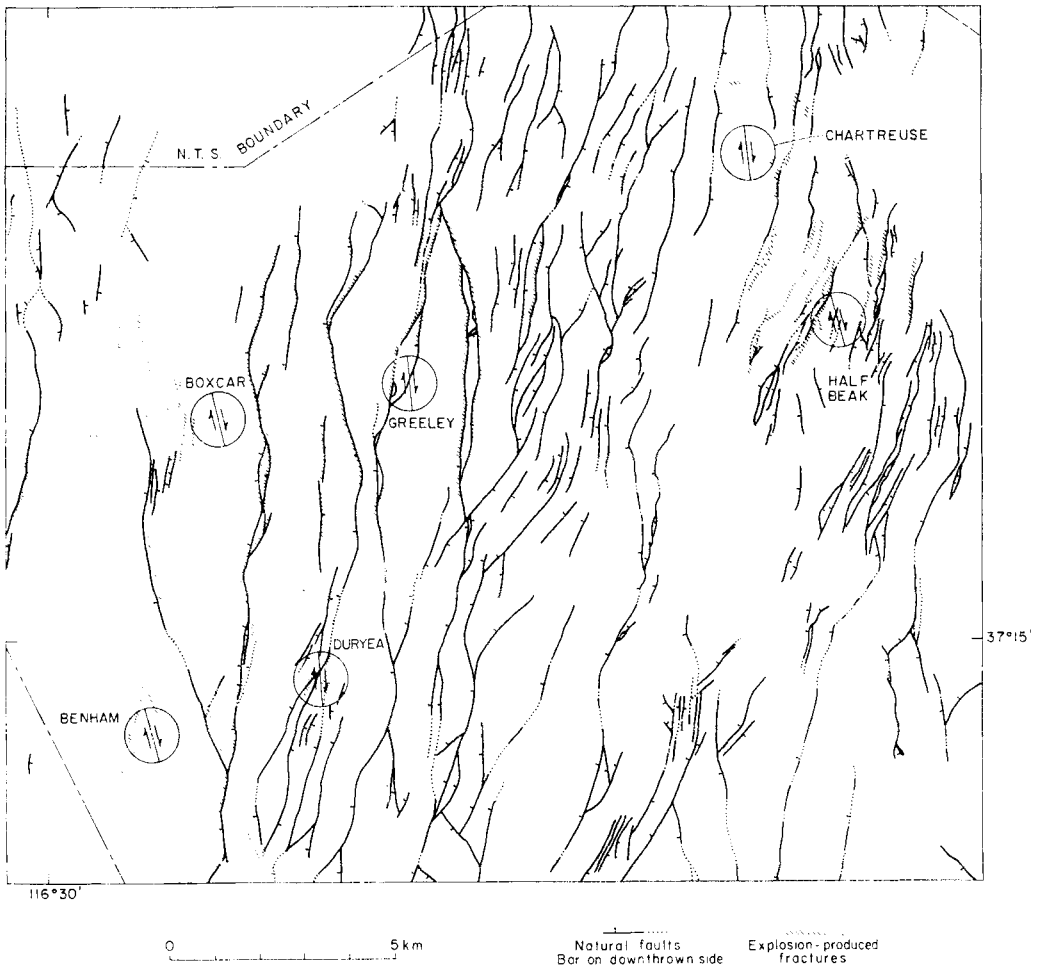

FIG. 9. Map of Pahute Mesa showing the fault plane orientations of the explosions studied, explosion-produced fractures, and natural faults in the area (faults after Orkild, Sargent & Snyder 1969).

(Hamilton & Healy 1969; Ryall & Savage 1969) as well as studies of faulting and fracturing caused by the explosions (Bucknam 1969; McKeown & Dickey 1969) have been published. Fig. 10 shows the relationships of these two sets of data with the source mechanisms determined for the two events. In the case of Benham, the correlation between the orientation of the double couple and the trend of the aftershock pattern as well as the orientation of faults and fractures is quite good. Both vertical and right-lateral movements on the nearby Boxcar fault were initiated by Benham.

The aftershocks of Benham were concentrated in two patterns (Hamilton & Healy 1969). Those to the north-west of ground zero follow a north-easterly trend while those to the west and south-west trend north–south. Fault plane solutions from *P* waves of events in the first group indicate dip-slip fault movement. Solutions for the second group indicate right-lateral strike-slip motion in a northerly direction. These two patterns were further confirmed in a study of smaller Benham aftershocks (Stauder 1971). The solutions for the second group of aftershocks are similar to the

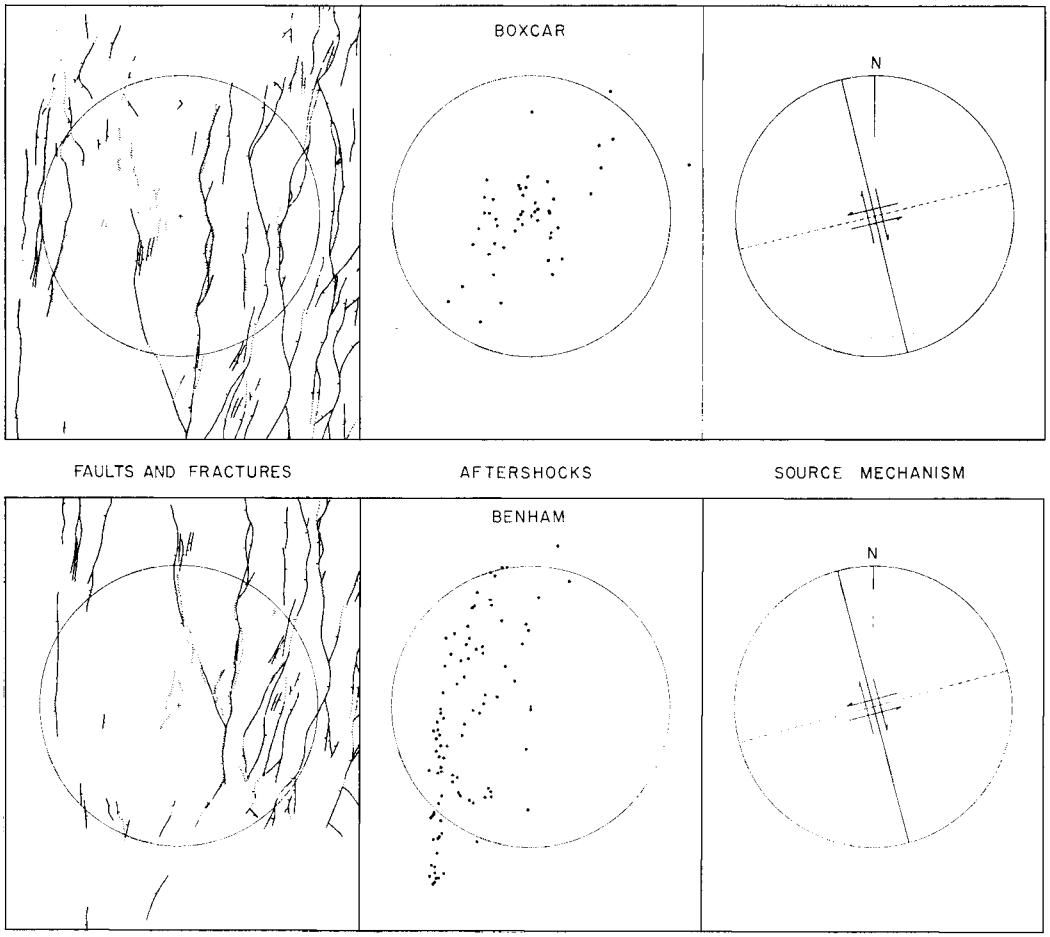

FIG. 10. Source mechanisms determined for the Boxcar and Benham events compared to natural faults and explosion-produced fracturing, and aftershock distribution. Aftershock distribution for Benham (Hamilton & Healy 1969), is that of the larger aftershocks (magnitude 3 to 4·2). Aftershocks from Boxcar (Ryall & Savage 1969) are those occurring in the first two days after the event. The circles are of radius 5 km centred on the ground zero of the explosion.

orientation of the double-couple component for Benham (and other events) as determined by this study. The Benham and Boxcar aftershocks when considered together (see Fig. 10) indicate the continuity of the distribution pattern. North-east-trending Benham aftershocks overlap with those of Boxcar.

3. Effect of tectonic strain release on magnitudes and discriminants

With explosions such as Pile Driver, Hardhat and Greeley where the surface wave energy due to strain release is greater than that of the explosion, one might expect the M_s values to increase. The expected theoretical increase ΔM_s determined from the Gutenberg–Richter energy-magnitude relationship for different F values is

Table 2

Effect of tectonic strain release on magnitudes

F Double-couple part	Energy ratio E_{tect}/E_{exp}	ΔM_s Maximum increase in magnitude due to tectonic component
0·3	0·12	0·07
0·5	0·33	0·08
0·7	0·65	0·14
1·0	1·33	0·24
1·5	3·00	0·40
2·0	5·33	0·53
3·0	12·00	1·08
4·0	21·33	1·23

listed in Table 2. These were computed using

$$\Delta M_s = \frac{1}{1{\cdot}6} \log (1 + E_{tect}/E_{exp}). \tag{5}$$

For explosions such as Pile Driver and Greeley (with F values of 3·2 and 1·6, respectively) one would expect surface wave magnitudes to be greater than those of corresponding explosions with small F values. One way of investigating this point is to look at M_s *vs.* m_b values for a series of explosions with different F values. In Fig. 11, $M_s - m_b$ explosion data from three different authors are plotted. Neither Pile Driver nor Greeley is distinguishable from the general explosion populations. The reason for this seems to be that Rayleigh waves due to the explosion component and double-couple component of the source reinforce and cancel out in alternate azimuthal quadrants. Thus when azimuthally averaged, the net effect on magnitudes is small.

To illustrate this point let us compare the Pile Driver radiation pattern and azimuthal range of the Canadian network stations used by Basham (1969) in his magnitude determinations in Fig. 12. With our source model, Canadian stations can be expected to record, on the average, normal Rayleigh wave amplitudes and thus yield a normal M_s *vs.* m_b value, as is indeed observed.

Thus to insure a representative magnitude, it is important to use data from several azimuths. Furthermore, while establishing station corrections for magnitude determinations, it is important to use data from explosions with low F values or from those at different sites.

4. Source-time function

All observations that have been made on the spectra of surface waves from explosions and earthquakes of comparable magnitudes indicate that earthquake spectra are richer in long-period components compared to explosions. This could be due to (a) source depth, (b) source volume, and (c) source-time function.

Tsai & Aki (1971) favour the source-depth effect to explain the differences in spectra while assuming the source function for explosions and earthquakes to be the same (step function). The spectra of deeper earthquakes would be shifted toward lower frequencies. This effect cannot be neglected but it does not explain two sets of data: (1) Some aftershocks of the Benham and Jorum events were accurately located.

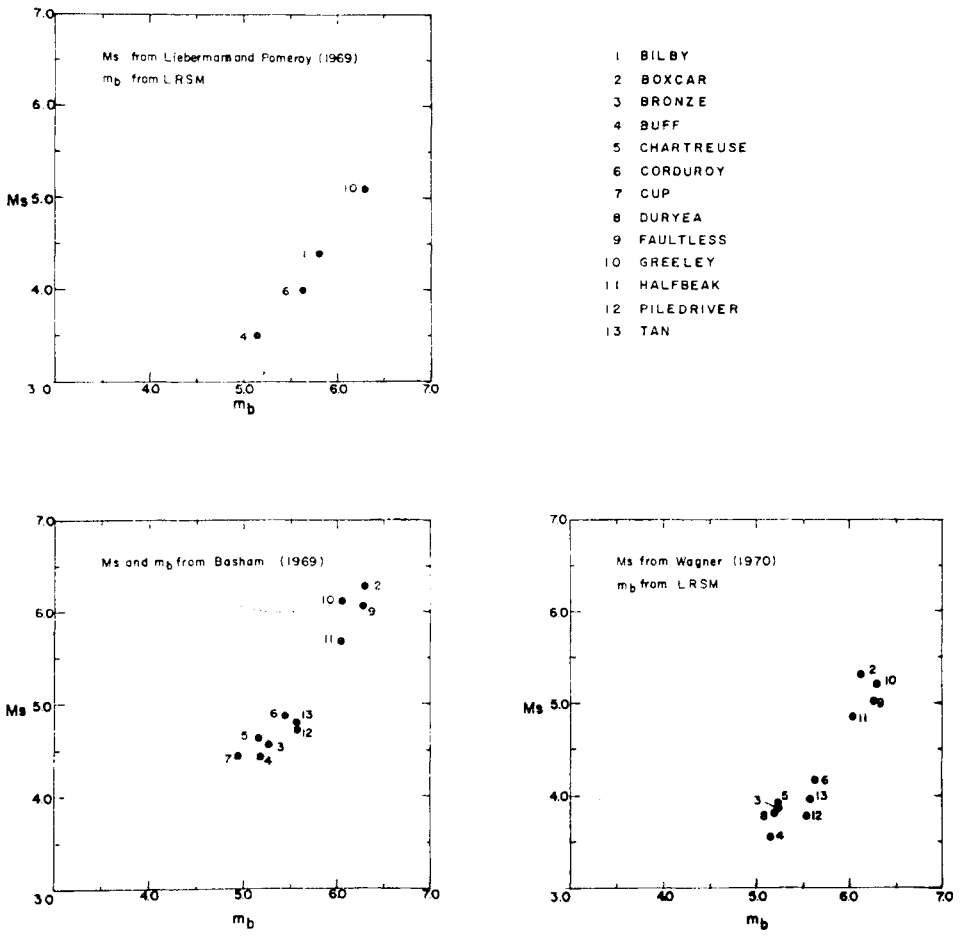

FIG. 11. $M_s - m_b$ for 13 American underground nuclear explosions from the data of Liebermann & Pomeroy (1969), Basham (1969), and Wagner (1970).

While focal depths were less than 5 km (some as shallow as 3·5 km) their spectral characteristics were similar to those of earthquakes rather than explosions (Molnar, *et al.* 1969; Savino *et al.* 1971). Also, spectra of collapse events are shifted toward lower frequencies relative to explosions. (2) Spectra of Love waves generated by the explosions are similar to those generated by earthquakes (Savino *et al.* 1971; Toksöz *et al.* 1971). In fact the Love wave source-time function determined from amplitude equalization is close to a step function.

For an explosion, a decaying source-pressure function, with or without a residual d-c pressure, could explain the observed spectra. In our earlier studies (Toksöz *et al.* 1964) we adopted a pressure function given by

$$p(t) = p_0 \, t \exp(-\eta t) \tag{6}$$

where p_0 is a constant and η is a time constant dependent on yield in a given medium. For Bilby, $\eta = 1{\cdot}5\,\mathrm{s}^{-1}$ fits the observed spectra at three stations as is shown in Fig. 13. Discrepancies at periods longer than $T = 30$ s are attributed to the effects of lateral heterogeneities and low signal-to-noise ratio.

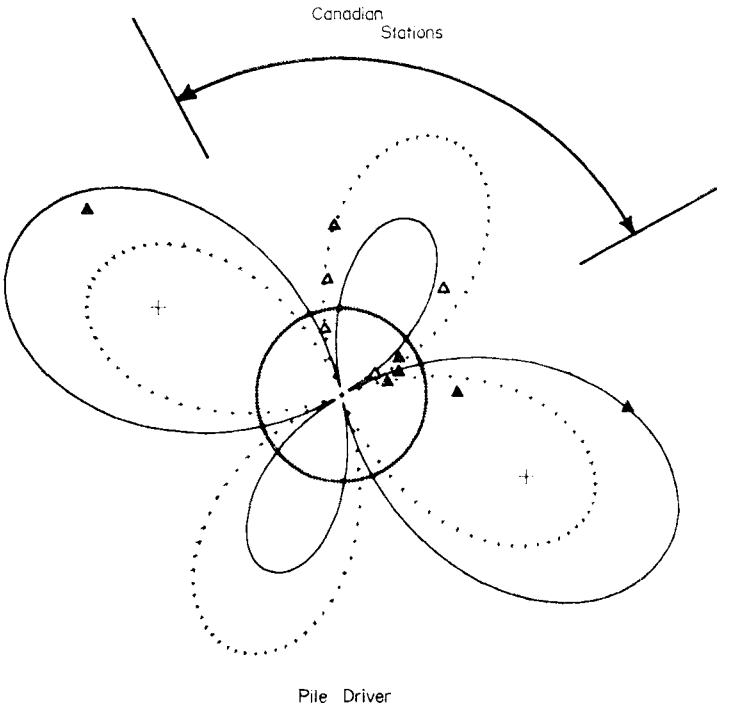

FIG. 12. Rayleigh wave radiation pattern for Pile Driver with the azimuthal range of Canadian stations from the event. △ LRSM stations with reversed polarity.

In a given medium, the source pulse becomes broader with increasing yield. This could be explained by the larger non-linear zone and hence greater attenuation of higher frequencies in this zone (Andrews & Shlien 1972). Observed ground displacement spectra of Rayleigh waves from several NTS explosions as recorded at LASA is shown in Fig. 14 along with three theoretical spectra for two source types. Curve 1 is based on a step function pressure variation. Curves 2 and 3 are based on the decaying pressure pulse with $\eta = 1$ and $\eta = 0{\cdot}6\,\mathrm{s}^{-1}$, respectively. It is clear that for the five lower explosions with intermediate yields, the decaying source function with $\eta = 1{\cdot}0$ fits the spectra, while for the three larger events, $\eta < 1$ is necessary. The spectra of the step function and the decaying pulse (equation (6)) type source functions are given by:

$$\left.\begin{aligned} |S(\omega)| &= \frac{1}{\omega} = T/2\pi && \text{step} \\ |S(\omega)| &= \frac{1}{\eta^2+\omega^2} = \frac{1}{\eta^2+(4\pi^2/T^2)} && \text{decaying pulse} \end{aligned}\right\} \quad (7)$$

where ω is the angular frequency and T is the period. At very low frequencies, the spectrum of the decaying pulse approaches a constant, while that of the step increases

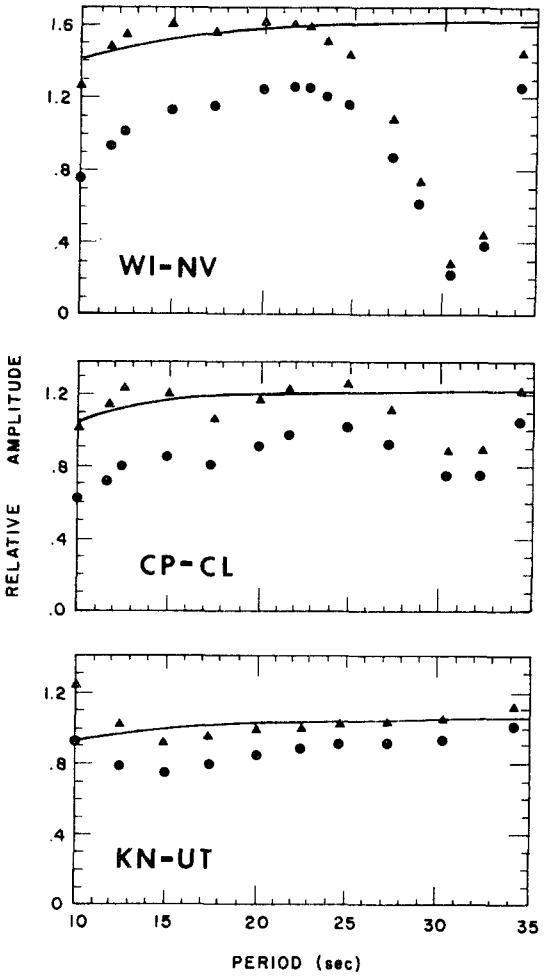

FIG. 13. Amplitude spectra of the source-time function for Bilby ($\eta = 1{\cdot}5\,s^{-1}$) at three stations after correction for propagation effects. Circles indicate data uncorrected for attenuation; triangles indicate the data corrected taking $Q = 100$.

with increasing period. At higher frequencies the pulse spectrum falls off proportionally to ω^{-2}, while the step falls off as $1/\omega$.

It has been observed that for small earthquakes and underground explosions with comparable Rayleigh wave amplitudes around $T = 20$ s, amplitudes in the longer period ranges around 40–60 s are considerably greater for the earthquakes than for the explosions (Molnar *et al.* 1969). This spectral difference, which serves as a discriminant, can be accounted for by the difference in source-time functions of the explosions (decaying pulse) and earthquakes (step function) as given in equation (7).

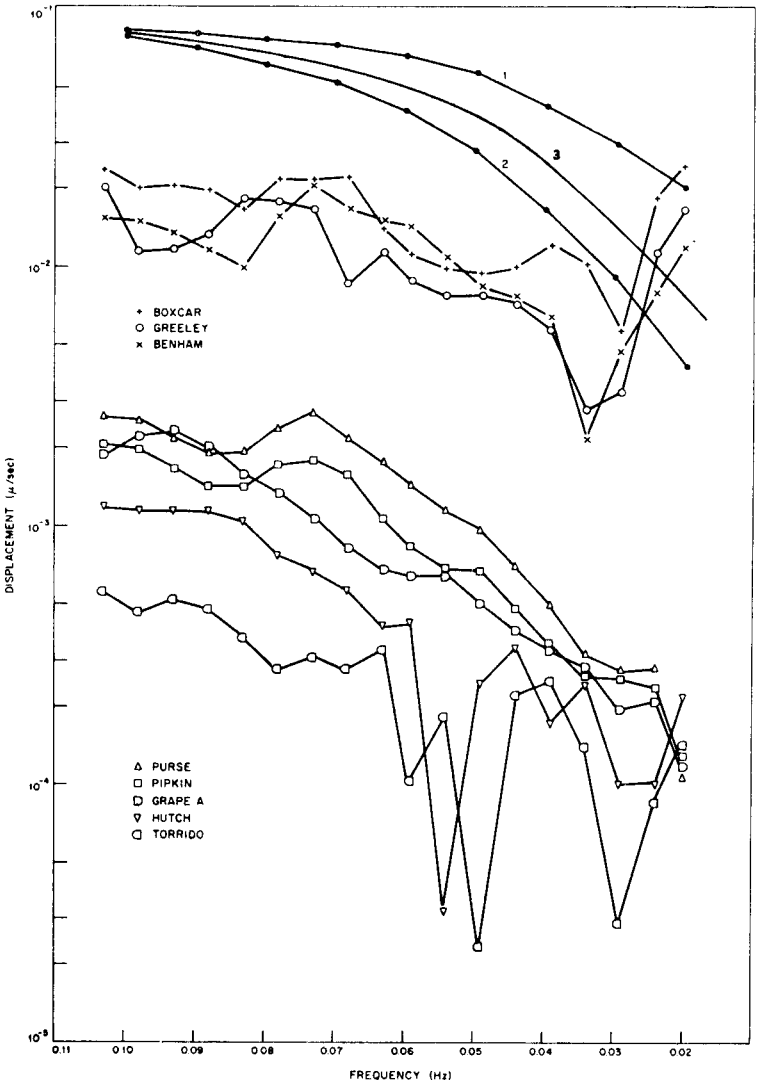

FIG. 14. Vertical component amplitude spectra, corrected for instrument response, from eight explosions recorded at LASA. Curves 1, 2, and 3 are computed Rayleigh wave spectra with different source time function: 1 = step function; 2 = decaying pulse, $\eta = 1{\cdot}0\,s^{-1}$; 3 = decaying pulse, $\eta = 0{\cdot}6\,s^{-1}$ (observed explosion spectra and Curves 1 and 2 from Lande & Filson 1970).

5. Conclusions

Nuclear explosions detonated in media with tectonic stresses interact with the ambient stress field and release some of the strain energy. This phenomenon complicates the Rayleigh wave radiation patterns and generates Love waves. It could also affect the $M_s - m_b$ discriminants. Some conclusions that can be derived from this study are:

1. The strain energy release from a particular explosion is dependent on the rock type and the state of stress in the medium. Generally, explosions in harder rocks release greater amounts of strain energy. This probably is related to the energy-storing

capability of these rocks. No significant Love waves have been observed from explosions in loose alluvium or salt domes.

2. In a given rock type tectonic strain energy release varies. As was shown by laboratory experiments (Toksöz *et al.* 1971), this is related to the ambient stress level.

3. The strength of the tectonic component of surface waves relative to the explosion itself generally increases with period.

4. Tectonic strain energy released as surface waves is generally less than the surface wave energy due to the explosion alone. In three cases (Pile Driver, Hardhat, and Greeley) the tectonic component of the surface waves exceeded those due to the explosion and, therefore, dominated the radiation pattern.

5. The tectonic strain release characteristics of explosions did not have significant effect on the $M_s - m_b$ discriminant. This may be due to two factors: (a) The mean Rayleigh wave amplitude when averaged over all azimuths, does not change as a result of the tectonic strain release component. Explosion and tectonic components of the source interfere constructively and destructively in alternating quadrants, and (b) Generally, for an explosion of given yield, the body wave amplitudes are larger when the source is in harder media. Thus, both M_s and m_b values could increase because of medium properties. Azimuthal averaging is most important for M_s in $M_s - m_b$ discrimination.

6. A decaying pulse-type source-time function is consistent with surface wave amplitude spectra in the 10- to 30-s period range. The shape of the pulse depends on medium properties and size of the explosion.

Acknowledgments

We thank Dr J. Filson for the LASA data and spectra. This research was supported by the Air Force Cambridge Research Laboratory under Contract No. F19628-72-C-0094 and by the Air Force Office of Scientific Research under Contract No. F44620-71-C-0049.

Department of Earth and Planetary Sciences
Massachusetts Institute of Technology
Cambridge, Massachusetts 02139

References

Aki, K., 1964. A note on surface waves from the Hardhat nuclear explosion, *J. geophys. Res.*, **69**, 1131–1134.

Aki, K., Reasenberg, P. DeFazio, T. & Tsai, Y., 1969. Near-field and far-field seismic evidence for triggering of an earthquake by the Benham explosion, *Bull. seism. Soc. Am.*, **59**, 2197–2209.

Andrews, D. J. & Shlien, S., 1972. Propagation of underground explosion waves in the nearly-elastic range, *EOS Transaction, Am. Geophys. Union*, **53**, abstract p. 451.

Archambeau, C. B., 1968. General theory of elastrodynamic source fields, *Rev. Geophys.*, **6**, 241–288.

Archambeau, C. B. & Sammis, C., 1970. Seismic radiation from explosions in prestressed media and the measurement of tectonic stress in the earth, *Rev. Geophysics.*, **8,** 473–499.

Barosch, P. J., 1968. Relationship of explosion-produced fracture patterns to geologic structure in Yucca Flats Nevada Test Site, in *Nevada Test Site*, ed. E. B. Eckel, *Geol. Soc. Am. Mem.*, **110,** 199–217.

Basham, P. W., 1969. Canadian magnitude of earthquakes and nuclear explosions in south-western North America, *Geophys. J. R. astr. Soc.*, **17,** 1–13.

Brune, J. N. & Pomeroy, P. W., 1963. Surface wave radiation patterns for underground nuclear explosions and small-magnitude earthquakes, *J. geophys. Res.*, **68,** 5005–5028.

Bucknam, R. C., 1969. Geologic effects of the Benham underground nuclear explosion, Nevada Test Site, *Bull. seism. Soc. Am.*, **59,** 2209–2220.

Canitez, N. & Toksöz, M. N., 1971. Focal mechanism and source depth of earthquakes from body- and surface-wave data, *Bull. seism. Soc. Am.*, **61,** 1369–1379.

Dickey, D. D., 1968. Fault displacement as a result of underground nuclear explosions, in *Nevada Test Site*, ed. E. B. Eckel, *Geol. Soc. Am. Mem.*, **110,** 219–232.

Dickey, D. D., 1969. Strain associated with the Benham underground nuclear explosion, *Bull. seism. Soc. Am.*, **59,** 2221–2230.

Dickey, D. D., 1971. Strain accompanying the Jorum underground nuclear explosion and its relation to geology, *Bull. seism. Soc. Am.*, **61,** 1571–1581.

Fernald, A. T., Corchary, C. S. & Williams, W. P., 1968. Surficial geologic map of Yucca Flat, Nye and Lincoln Counties, Nevada, *U.S. Geol. Survey Misc. Geol. Inv. Map I-550.*

Hamilton, R. M. & Healy, J. H., 1969. Aftershocks of the Benham nuclear explosion, *Bull. seism. Soc. Am.*, **59,** 2271–2281.

Harkrider, D. G., 1964. Surface waves in multilayered elastic media, 1. Rayleigh and Love waves from buried sources in a multilayered elastic half-space, *Bull. seism. Soc. Am.*, **54,** 627–680.

Kehrer, H. H., 1969. *Radiation patterns of seismic surface waves from nuclear explosions*, M.S. Thesis, Massachusetts Institute of Technology, Cambridge, Massachusetts.

Lande, L. & Filson, J., 1971. Scaled Rayleigh wave spectra from explosions, Semiannual Tech. Summary-Seismic Discrimination, *M.I.T. Lincoln Laboratory*, 1–3, 8–11.

Leavy, D., 1971. *Scattering of elastic waves around a compressional source*, M.S. Thesis, Massachusetts Institute of Technology, Cambridge, Massachusetts.

Liebermann, R. C. & Pomeroy, P. W., 1969. Relative excitation of surface waves by earthquakes and underground explosions, *J. geophys. Res.*, **74,** 1575–1590.

McKeown, F. A. & Dickey, D. D., 1969. Fault displacements and motion related to nuclear explosions, *Bull. seism. Soc. Am* , **59,** 2253–2269.

McKeown, F. A., Orkild, P. P., Dickey, D. D. & Snyder, R. P., 1966. Some geologic data pertinent to the seismic characteristics of Pahute Mesa, *USGS Tech.-Letter: Sp. Std. I-45.*

Molnar, P., Jacob, K. & Sykes, L. R., 1969. Microearthquake activity in eastern Nevada and Death Valley, California before and after the nuclear explosion Benham, *Bull. seism. Soc. Am.*, **59,** 2177–2184.

Molnar, P., Savino, J., Sykes, L. R., Liebermann, R. C., Hade, G. & Pomeroy, P. W., 1969. Small earthquakes and explosions in western North America recorded by new high gain, long period seismographs, *Nature*, **224,** 1268–1273.

Orkild, P. P., Sargent, K. A. & Snyder, R. P., 1969. Geologic map of Pahute Mesa, Nevada Test Site, Nye County, Nevada, *U.S. Geol. Survey Misc. Geol. Inv. Map I-567.*

Press, F. & Archambeau, C. B., 1962. Release of tectonic strain by underground nuclear explosions, *J. geophys. Res.*, **67,** 337–343.

Ryall, A. & Savage, W. U., 1969. A comparison of seismological effects for the Nevada underground test Boxcar with natural earthquakes in the Nevada region, *J. geophys. Res.*, **74,** 4281–4289.

Savino, J., Sykes, L. R., Liebermann, R. C. & Molnar, P., 1971. Excitation of seismic surface waves with periods of 15 to 70 seconds for earthquakes and underground explosions, *J. geophys. Res.*, **76,** 8003–8020.

Stauder, W., 1971. Smaller aftershocks of the Benham nuclear explosion, *Bull. seism. Soc. Am.*, **61,** 417–428.

Toksöz, M. N., 1967. Radiation of seismic surface waves from underground explosions, *Proceedings of the Vesiac Conference on the current status and future prognosis of shallow seismic events,* VESIAC Rept., Willow Run Laboratories, The University of Michigan, 65–84.

Toksöz, M. N., Ben-Menahem, A. & Harkrider, D. G., 1964. Determination of source parameters by amplitude equalization of seismic surface waves, 1. Underground nuclear explosions, *J. geophys. Res.*, **69,** 4355–4366.

Toksöz, M. N., Harkrider, D. G. & Ben-Menahem, A., 1965. Determination of source parameters by amplitude equalization of seismic surface waves, 2. Release of tectonic strain by underground nuclear explosions and mechanisms of earthquakes, *J. geophys. Res.*, **70,** 907–922.

Toksöz, M. N. & Kehrer, H. H., 1971. Underground nuclear explosions: tectonic utility and dangers, *Science*, **173,** 230–233.

Toksöz, M. N., Thomson, K. C. & Ahrens, T. J., 1971. Generation of seismic waves by explosions in prestressed media, *Bull. seism. Soc. Am.*, **61,** 1589–1623.

Tsai, Y. & Aki, K., 1971. Amplitude spectra of surface waves from small earthquakes and underground nuclear explosions, *J. geophys. Res.*, **76,** 3940–3952.

Wagner, D. E., 1970. Nuclear yields from Rayleigh waves, *Earthquake Notes*, **41,** 9–20.